Published in final edited form as:
Cancer Prev Res (Phila). 2010 August ; 3(8): 1015–1025. doi:10.1158/1940-6207.CAPR-10-0020.

Cryptotanshinone inhibits cancer cell proliferation by suppressing mTOR-mediated cyclin D1 expression and Rb phosphorylation

Wenxing Chen[1,4], **Yan Luo**[1], **Lei Liu**[1], **Hongyu Zhou**[1], **Baoshan Xu**[1], **Xiuzhen Han**[1], **Tao Shen**[1], **Zhijun Liu**[3], **Yin Lu**[4], and **Shile Huang**[1,2,*]

[1]Department of Biochemistry and Molecular Biology, Louisiana State University Health Sciences Center, 1501 Kings Highway, Shreveport, LA 71130-3932, USA

[2]Feist-Weiller Cancer Center, Louisiana State University Health Sciences Center, 1501 Kings Highway, Shreveport, LA 71130-3932, USA

[3]School of Renewable Natural Resources, Louisiana State University, Baton Rouge, LA 70803, USA

[4]Nanjing University of Chinese Medicine, 282 Hanzhong Road, Nanjing, Jiangsu Province, China

Abstract

Cryptotanshinone (CPT), a natural compound isolated from the plant *Salvia miltiorrhiza* Bunge, is a potential anticancer agent. However, little is known about its anticancer mechanism. Here we show that CPT inhibited cancer cell proliferation by arresting cells in G_1/G_0 phase of the cell cycle. This is associated with inhibiting expression of cyclin D1 and phosphorylation of retinoblastoma (Rb) protein. Furthermore, we found that CPT inhibited the signaling pathway of the mammalian target of rapamycin (mTOR), a central regulator of cell proliferation. This is evidenced by the findings that CPT inhibited type I insulin-like growth factor (IGF-1) or 10% fetal bovine serum (FBS)-stimulated phosphorylation of mTOR, p70 S6 kinase 1 (S6K1) and eukaryotic initiation factor 4E (eIF4E) binding protein 1 (4E-BP1), in a concentration- and time-dependent manner. Expression of constitutively active mTOR conferred resistance to CPT inhibition of cyclin D1 expression and Rb phosphorylation, as well as cell growth. The results suggest that CPT is a novel anti-proliferative agent.

Keywords

cryptotanshinone; cyclin D1; mTOR; cell cycle; proliferation

Introduction

Deregulation of cell cycle progression plays an important role in the development of cancer (1). Cell cycle progression occurs in an orderly fashion and is tightly regulated by the expression and activity of cyclin/cyclin-dependent kinase (CDK) complexes (1,2). The CDK complexes can be activated at specific points of the cell cycle when a CDK is bound with cyclins, or inactivated when CDK inhibitors bind the CDK (1,2). Of cyclins, cyclin D1 is critical in controlling cell cycle progression from G_1 to S phase (2,4). Cyclin D1 binds to CDK4/6 and forms the cyclin/CDK complexes, which result in phosphorylation and activation of the CDKs

[*]**Correspondence to:** Shile Huang, Ph.D., Department of Biochemistry and Molecular Biology, Louisiana State University Health Sciences Center, 1501 Kings Highway, Shreveport, LA 71130-3932, USA. Fax: +318-675-5180. shuan1@lsuhsc.edu.

(1). Subsequently, the activated CDKs phosphorylate the retinoblastoma (Rb) tumor suppressor protein (5). Hypophosphorylated Rb binds E2F, suppressing the transcription activity of E2F; whereas phosphorylated Rb is released from E2F, promoting transition from G_1 to S phase (5). Therefore, the Rb protein has an essential role in mediating G_1 progression through the restriction point.

The mammalian target of rapamycin (mTOR), a Ser/Thr kinase, lies downstream of the type I insulin-like growth factor (IGF-1) receptor-phosphatidylinositol 3′ kinase (PI3K) (6). Recently, two mTOR complexes (mTORC1 and mTORC2) have been identified in mammalian cells (6). mTORC1 is composed of mTOR, mLST8 (also termed G-protein β-subunit-like protein, GβL, a yeast homolog of LST8), PRAS40 (proline-rich Akt substrate 40 kDa) and raptor (regulatory-associated protein of mTOR), and is rapamycin-sensitive (7–13). In response to growth factors and nutrients, mTORC1 regulates cell proliferation and growth by controlling protein (cyclin D1, ornithine decarboxylase, etc.) synthesis and ribosome biogenesis through phosphorylation of downstream effectors like 4E-BP1 (eukaryotic initiation factor 4E binding protein 1) and S6K1 (ribosomal p70 S6 kinase 1) (7–14). mTORC2 consists of mTOR, mLST8, mSin1 (mammalian stress-activated protein kinase-interacting protein 1), rictor (rapamycin insensitive companion of mTOR), protor (protein observed with rictor) and PRR5 (proline-rich protein 5), and is rapamycin-insensitive (15–21). mTORC2 phosphorylates Akt and PKC, signals to small GTPases (RhoA and Rac1), and controls cytoskeleton organization (17,22–25). Though the cellular functions of the mTOR complexes remain to be determined, current data indicate that mTOR is a key kinase in the regulation of cell proliferation, growth, survival, differentiation, motility and angiogenesis (6,14).

Cryptotanshinone (CPT) is one of the major tanshinones isolated from *Salvia miltiorrhiza* Bunge (Danshen) that has been used in traditional oriental medicine for treatment of a variety of diseases including coronary artery disease (26), hyperlipidemia (27), acute ischemic stroke (27), and chronic renal failure (28), chronic hepatitis (29), and Alzheimer's disease (30). Studies have shown that CPT inhibits inflammation by suppressing cyclooxygenase-2 (COX-2) activity (31); inhibits TNF-α-induced matrix metalloproteinase-9 production and migration in human aortic smooth muscle cells via downregulation of NF-κB and AP-1 (32); acts against diabetes and obesity via activating AMP-activated protein kinase (33). CPT inhibits chemotactic migration in macrophages through blocking PI3K signaling (34), but protects primary rat cortical neurons from glutamate-induced neurotoxicity via activating PI3K/Akt signaling (35). Most recent studies have shown that CPT is also a potential anticancer agent (36,37). Though CPT has been found to inhibit prostate cancer cell growth by inactivating the signal transducer and activator of transcription 3 (Stat3) activity (37), the anticancer mechanism of CPT remains to be elucidated.

Here we show that CPT inhibited the growth of a panel of tumor cell lines by arresting cells in G_1/G_0 phase of the cell cycle. Concurrently, CPT inhibited expression of cyclin D1 and phosphorylation of Rb protein. Further, we found that this is related to inhibition of mTOR signaling pathway.

Materials and Methods

Materials

Cryptotanshinone (CPT), tanshinone I, tanshinone IIA, dihydrotanshinone were extracted from the roots of Salvia miltiorrhiza Bunge (Danshen) using ethanol. Briefly, the root (200 g) of Danshen or red sage (*Salvia miltiorrhiza*) was extracted with 2 L 95% aqueous ethanol in a high-power blending extractor for 10 min. After the extraction, the supernatant solution was filtered through a filter paper (Whatman #4). The filtrate was freed of ethanol under reduced pressure and lyophilized to powder (10.95 g). The ethanol extract yield was approximately

5.5% (w/w). HPLC chromatographic fingerprints showed that the ethanol extract of Danshen contained numerous components including the water-soluble salvianolic acid B and the water-insoluble tanshinones including the indicated four compounds. The four tanshinone compounds were purified by HPLC (>95% purity for dihydrotanshinone, and >98% purity for CPT, tanshinone I and tanshinone IIA), and were dissolved in 100% ethanol to prepare stock solutions (20 mM), which were aliquoted and stored at −20°C.

RPMI 1640 and Dulbecco's Modified Eagle Medium (DMEM) were purchased from Mediatech (Herndon, VA, USA). Fetal bovine serum (FBS) was from Hyclone (Logan, UT, USA), and 0.05% Trypsin-EDTA from Invitrogen (Grand Island, NY, USA). Type I insulin-like growth factor (IGF-1) (PeproTech, Rocky Hill, NJ, USA) was rehydrated in 0.1 M acetic acid to prepare a stock solution (10 μg/ml), aliquoted and stored at −80°C. Enhanced chemiluminescence solution was from Perkin Elmer Life Science (Boston, MA, USA). CellTiter 96® AQ_{ueous} One Solution Cell Proliferation Assay kit was from Promega (Madison, WI, USA). The following antibodies were used: 4E-BP1 (Zymed, South San Francisco, CA, USA), Akt, p-S6K1 (Thr389), S6K1, cyclin D1, Rb, p-Rb (Ser780), CDK2, CDK4 (Santa Cruz Biotechnology, Santa Cruz, CA, USA), phospho-Akt (Ser473, Thr308), phospho-mTOR (Ser2448), mTOR (Cell Signaling, Beverly, MA, USA), AU1 (Bethyl Laboratories, Montgomery, TX, USA), β-tubulin (Sigma, St. Louis, MO, USA), goat anti-mouse IgG-horseradish peroxidase and goat anti-rabbit IgG-horseradish peroxidase (Pierce, Rockland, IL, USA).

Cell lines and cultures

Human rhabdomyosarcoma (Rh30) cell line expressing mutant *p53* alleles R273C (38) was generously provided by Dr. Peter J. Houghton (St. Jude Children's Research Hospital, Memphis, TN, USA). Human prostate carcinoma (DU145) and breast carcinoma (MCF-7) cells were from American Type Culture Collection (Manassas, VA, USA). Rh30 and DU145 cells were grown in antibiotic-free RPMI 1640 medium supplemented with 10% FBS, whereas MCF-7 cells were grown in antibiotic-free DMEM supplemented with 10% FBS. All cells were maintained in a humid incubator (37°C, 5% CO_2). For experiments where cells were deprived of serum, cell monolayers were washed with phosphate-buffered saline (PBS) and incubated in the serum-free DMEM.

One solution cell proliferation assay

Cell proliferation was evaluated using The CellTiter 96® AQueous One Solution Cell Proliferation Assay (Promega), which is a colorimetric method to determine the number of viable cells in proliferation or cytotoxicity. Briefly, cells suspended in the growth medium were seeded in a 96-well plate at a density of 1×10^4 cells/well (in 6 replicates) and were grown overnight at 37°C in a humidified incubator with 5% CO_2. Next day, CPT, tanshinone I, tanshinone IIA or dihydrotanshinone (0–40 μM) was added. After incubation for 48 h, each well was added 20 μl of one solution reagent (Promega) and incubated for 4 h. Cell proliferation was determined by measuring the optical density (OD) at 490 nm using a Wallac 1420 Multilabel Counter (Perkin-Elmer Life Sciences, Wellesley, MA, USA).

[^{3}H]Thymidine incorporation assay

[^{3}H]Thymidine incorporation assay was performed as described (39). Briefly, Rh30 or DU145 cells (3×10^4 cells/well) were seeded in 48-well plates in triplicate with 10% FBS-RPMI 1640 medium and were grown overnight at 37°C in a humidified incubator with 5% CO_2. Next day, CPT (0–40 μM) was added. After incubation for 48 h, methyl-[^{3}H] thymidine (1 μCi/well) (Amersham Biosciences, Piscataway, NJ, USA) was added. Following incubation for 8 h at 37°C, the used medium was aspirated. Subsequently, the cells were briefly washed with cold PBS, and then incubated with ice cold 5% trichloroacetic acid for 30 min at 4°C. After a wash

with PBS, the cells were incubated with 0.5M NaOH/0.5% SDS (250 μl/well) for 1 h. Finally, the activity of [^{3}H] thymidine incorporated was measured by a LS6500 scintillation counter (Beckman Coulter, Brea, CA, USA).

Cell cycle analysis

Cell cycle analysis was performed as described previously (38). Briefly, cells were seeded in 100-mm dishes at a density of 1×10^6 cells/dish in the growth medium and were grown overnight at 37°C in a humidified incubator with 5% CO_2. After treatment with CPT (0–40 μM) for 24 h, the cells were briefly washed with PBS and trypsinized. Cell suspensions were centrifuged at 1,000 rpm for 5 min, and pellets were stained with the Cellular DNA Flow Cytometric Analysis Kit (Roche Diagnostics Corp., Indianapolis, IN, USA). Percentages of cells within each of the cell cycle compartments (G_0/G_1, S, or G_2/M) were determined by flow cytometry (FACSCalibur; Becton Dickinson, Mountain View, CA, USA). Cells treated with vehicle alone (100% ethanol) were used as a control.

Expression of constitutively active mTOR by adenoviral infection of cells

Recombinant adenovirus encoding AU1-tagged constitutively active mTOR (Ad-mTOR-RD) was a gift from Dr. Christopher J. Rhodes (Pacific Northwest Research Institute, Seattle, WA, USA) (40). The virus was amplified and titrated as described previously (41). For experiments, Rh30 cells were grown in 6-well plates with RPMI 1640 supplemented with 10% FBS, and infected with Ad-mTOR-RD for 24 h at the multiplicity of infection of 5. Subsequently, cells were serum-starved for 24 h, and then treated with or without CPT (20 μM) for 2 h, followed by stimulation with or without IGF-1 (10 ng/ml) for 1 h. Cells infected with Ad-GFP, encoding the green fluorescence protein (GFP) (42), served as a control. Expression of AU1-tagged constitutively active mTOR was confirmed by Western blotting with antibodies to AU1, p-S6K1, 4E-BP1 and β-tubulin.

Western blot analysis

Western blotting was performed as described previously (38). Briefly, following treatment, cells were washed with cold PBS. On ice, cells were lysed in RIPA buffer, containing 50 mM Tris, pH 7.2; 150 mM NaCl; 1% sodium deoxycholate; 0.1% SDS; 1% Triton-X 100; 10 mM NaF; 1 mM Na_3VO_4; protease inhibitor cocktail (1:1000, Sigma, St. Louis, MO, USA). Lysates were sonicated for 10 s and centrifuged at 14,000 rpm for 10 min at 4°C. Protein concentration was determined by bicinchoninic acid assay with bovine serum albumin as standard (Pierce, Rockford, IL, USA). Equivalent amounts of protein were separated on 7.5%–12% SDS-polyacrylamide gel and transferred to polyvinylidene difluoride membranes (Millipore, Bedford, MA, USA). Membranes were incubated with PBS containing 0.05% Tween 20 and 5% nonfat dry milk to block nonspecific binding and were incubated with primary antibodies, then with appropriate secondary antibodies conjugated to horseradish peroxidase. Immunoreactive bands were visualized by using Renaissance chemiluminescence reagent (Perkin-Elmer Life Science, Boston, MA, USA).

Statistical analysis

Results were expressed as mean values ± standard error (mean ± SE). The data were analyzed by one-way analysis of variance (ANOVA) followed by post-hoc Dunnett's *t*-test for multiple comparisons. A level of $P < 0.05$ was considered to be significant.

Results

CPT inhibits cancer cell proliferation

To assess the anti-proliferative activities of CPT, tanshinone I, tanshinone IIA and dihydrotanshinone CPT, one solution assay was used. As shown in Fig.1A, treatment with the compounds for 48 h inhibited the growth of rhabdomyosarcoma (Rh30) and prostate cancer (DU145) cells in a concentration-dependent manner. Of the compounds, only CPT potently inhibited the growth of the cells at low micromolar concentrations (2.5–10 μM). The IC_{50} values of CPT were approximately 5.1 μM in Rh30, and 3.5 μM in DU145 cells, respectively, whereas the IC_{50} values of dihydrotanshinone, tanshinone I, and tanshinone IIA were > 20 μM in both Rh30 and DU145 cells. Similar data were also observed in MCF-7 cells (data not shown). The data suggest that CPT, among the tanshinones, is the most potent anti-proliferative agent.

Because the one solution assay, in fact, determines the number of viable cells in proliferation or cytotoxicity, to confirm the inhibitory effects of CPT on cell proliferation, we have also performed [^{3}H]thymidine incorporation assay. As shown in Fig.1B, CPT did inhibit [^{3}H] thymidine incorporation in Rh30 and DU145 cells in a concentration dependent manner. The IC_{50} values of CPT were approximately 8.5 μM in Rh30, and 5.2 μM in DU145 cells, respectively. The data indicate that CPT does inhibit tumor cell proliferation.

CPT arrests cells in G_1/G_0 phase of the cell cycle by inhibiting Cyclin D1 expression and Rb phosphorylation

Cell proliferation is controlled by the progression of the cell cycle (1). To understand how CPT inhibits cell proliferation, the effect of CPT on cell-cycle distribution was assessed using the Cellular DNA Flow Cytometric Analysis Kit (Roche Diagnostics Corp.) and flow cytometry. We found that treatment with CPT for 24 h arrested Rh30 and DU145 cells in G_1/G_0 phase of the cell cycle in a concentration-dependent manner, consistent with the results shown in Fig. 1. At 10 μM, CPT treatment significantly increased the proportion of Rh30 cells in the G_1/G_0 phase from 44.28% to 60.33% (Fig.2A). This increase in G_1/G_0 cell population was accompanied with a concomitant decrease of cell number in S-phase or G_2/M phase of the cell cycle (Fig.2B). Prolonged treatment (48 h) with CPT did not significantly enhance the proportion of Rh30 cells in the G_1/G_0 phase (e.g. at 10 μM, 60.33% for 24 h *vs.* 61.87% for 48 h) (data not shown). Similar results were observed in DU145 cells, even treated with CPT for up to 96 h (see Supplimentary data, Fig.S1), indicating that CPT inhibition of cell proliferation is attributed to the induction of G_1/G_0 cell cycle arrest.

Cyclins and CDKs play an essential role in the regulation of cell cycle progression (1). Thus, perturbation of cyclins or CDKs expression may contribute to the altered cell cycle distribution. Of the cell-cycle related cyclins, cyclins D and E play an important role in the transition from the G_1 to S phase, and cyclin D1-CDK4/6 and cyclin E-CDK2 complexes are required for G_1 progression (1). Since CPT induced G_1/G_0 cell-cycle arrest, next we examined protein expression of cyclin A, cyclin B1, cyclin D1, cyclin E, CDK2, and CDK4. As shown in Fig. 3, treatment of Rh30 with CPT for 24 h inhibited cellular protein expression of cyclin D1 in a concentration-dependent manner. Starting at 10 μM, CPT reduced expression of cyclin D1 sharply. Protein levels of other molecules including cyclin A, cyclin B1, cyclin E, CDK2, and CDK4 were not obviously altered (Fig.3). As Rb, one of the most important G_1 phase cyclin/CDK substrates, functions as an archetypal tumor suppressor and a regulator of cell cycle progression in the late G_1 phase (2), we investigated the effect of CPT on Rb phosphorylation. As shown in Fig.3, Rb was expressed as a 110-kDa band on Western blotting in vehicle treated control Rh30 cells. After 10 μM CPT treatment for 24 h, a lower band, which migrates rapidly and represents the dephosphorylated protein, was observed, indicating that CPT inhibits

phosphorylation of Rb (Fig.3). The status of Rb phosphorylation is closely related to the level of cyclin D1. Similar results were observed in DU145 cells (see Supplementary data, Fig.S2). The data suggest that CPT arrests cells in G_1/G_0 phase of the cell cycle by inhibiting cyclin D1 expression and Rb phosphorylation, which is not cell type-dependent.

CPT inhibits mTOR signaling pathway

mTOR plays a central role in the regulation of cell proliferation and growth (6,14). Inhibition of mTOR by rapamycin downregulates cyclin D1 expression (43) and Rb phosphorylation (44), resulting in cell cycle arrest in G_1/G_0 phase. Since we found that CPT arrested cells in G_1/G_0 phase of the cell cycle by inhibiting cyclin D1 expression and Rb phosphorylation, we hypothesized that CPT may inhibit mTOR signaling pathway. To test this hypothesis, we set out to examine the effect of CPT on mTOR signaling in Rh30 and DU145 cells. As mTOR signaling can be activated by nutrients, hormones and growth factors, such as insulin and IGF-1 (6), we therefore first investigated the effect of CPT on mTOR signaling in IGF-1-stimulated cells. The results indicate that treatment of serum-starved Rh30 cells with CPT for 2 h inhibited IGF-1-stimulated phosphorylation of S6K1 and 4E-BP1, the two best characterized downstream effector molecules of mTORC1 (6), in a dose- and time-depedent manner (Fig. 4A). After 2 h exposure, CPT remarkably suppressed IGF-1-stimulated phosphorylation of S6K1 (Thr389) starting at 2.5 μM (Fig.4A); and at 10 μM, CPT dramatically inhibited this phosphorylation event within 2 h in Rh30 cells (Fig.4A). No obvious effect of CPT on total protein levels of S6K1 was detected using an anti-S6K1 antibody that recognizes both phosphorylated and unphosphorylated forms (Fig.4A). Similarly, the effect of CPT on phosphorylation state of 4E-BP1 was detected with an antibody to 4E-BP1. Phosphorylation of 4E-BP1 decreases its electrophoretic mobility during SDS-polyacrylamide gel electrophoresis (45). CPT inhibited IGF-1-stimulated phosphorylation of 4E-BP1 in Rh30 cells, as indicated by the decrease in the intensity of the uppermost band γ and by the increase in the higher mobility band α that corresponds to a less phosphorylated form of 4E-BP1 (Fig. 4A). In addition, we found that CPT also inhibited IGF-1-stimulated phosphorylation of mTOR at Ser2448, a site phosphorylated by S6K1 (46), in a dose- and time-dependent manner (Fig. 4A). Similar data were also observed in DU145 and MCF-7 cells (data not shown), and Rh30 cells grown in the normal culture medium containing 10% FBS (Fig.4B). Moreover, we found that CPT analogs, including tanshinone I, tanshinone IIA and dihydrotanshinone, did not obviously alter phosphorylation of S6K1, 4E-BP1 and mTOR (Fig.4C), which is consistent with the findings that CPT, but not tanshinone I, tanshinone IIA and dihydrotanshinone, potently inhibited cancer cell growth.

mTOR functions as two complexes, mTORC1 and mTORC2, which phosphorylate S6K1/4E-BP1 and Akt, respectively (17,18,22). After demonstrating that CPT inhibits mTORC1-mediated phosphorylation of S6K1 and 4E-BP1, we further tested whether CPT inhibits mTORC2-mediated phosphorylation of Akt. To our surprise, CPT increased phosphorylation of Akt (S473 and T308) in Rh30 cells and DU145 cells in a concentration-dependent manner (Fig.5). Taken together, our data suggest that CPT may represent a novel inhibitor for mTORC1, but not for mTORC2.

Expression of constitutively active mTOR confers high resistance to CPT inhibition of mTOR signaling, cyclin D1 expression and Rb phosphorylation

mTOR regulates cyclinD1 expression and Rb phosphorylation, and inhibition of mTOR by rapamycin arrests cells in G_1/G_0 phase of the cell cycle (43,44). To determine whether CPT inhibition of cyclin D1 expression and Rb phosphorylation is due to inhibition of mTOR signaling, Rh30 cells were infected with recombinant adenovirus expressing AU1-tagged constitutively active mTOR (mTOR-RD). We found that ectopic expression of constitutively active mTOR increased the basal level of phosphorylation of S6K1, but not Akt, in serum-

starved Rh30 cells (Fig.6A), suggesting that the constitutively active mTOR was functional in the cells. Of interest, treatment with CPT (10 μM) for 24 h inhibited the basal or IGF-1-stimulated S6K1 phosphorylation, as well as cyclin D1 expression and Rb phosphorylation in the cells infected with Ad-GFP (Fig.6A), which is consistent with the data seen in the parental Rh30 cells (Fig.3). However, expression of constitutively active mTOR conferred high resistance to CPT inhibition of S6K1 phosphorylation, as well as cyclin D1 expression and Rb phosphorylation (Fig.6A). The results suggest that CPT inhibits cyclin D1 expression and Rb phosphorylation through targeting mTOR signaling.

Expression of constitutively active mTOR partially prevents CPT inhibition of cancer cell growth

To further determine the role of mTOR in CPT inhibition of cell growth, Rh30 cells were infected with Ad-GFP (control) and Ad-mTOR-RD. Expression of constitutively active mTOR, but not GFP, rendered partial resistance to CPT inhibition of cell growth. This is evidenced by cell counting (Fig.6B) and cell cycle analysis (Fig.6C). Expression of constitutively active mTOR significantly prevented CPT (5–20 μM) inhibition of cell growth by 1.4~2.2-fold (Fig.6B). Cell cycle analysis reveals that expression of constitutively active mTOR also significantly attenuated CPT induction of G_1/G_0 cell cycle arrest (Fig.6C). Similar data were observed in DU145 cells (see Supplementary data, Fig.S3).The results suggest that CPT inhibits cancer cell growth at least partially through inhibiting mTOR signaling.

Discussion

In this study, we observed that CPT inhibited cell proliferation by arresting the cell cycle in G_1/G_0 phase in rhabdomyosarcoma (Rh30), prostate (DU145) and breast (MCF-7) cancer cells. This is related to CPT arresting cells in G_1/G_0 phase by inhibiting expression of cyclin D1 and phosphorylation of Rb protein. Of importance, here for the first time we show that the anti-proliferative effect of CPT is associated with inhibition of the signaling pathway of mTOR, a master kinase that regulates cell proliferation (6,14), suggesting that CPT may be a new mTOR inhibitor. Further understanding the underlying mechanism may lead to design of novel tumor-selective therapeutics. Recent studies have shown that CPT inhibits prostate cancer cell growth by inhibiting phosphorylation of Stat3 in JAK2-indepdent mechanism (37). It has been suggested that Stat3 is positively regulated by mTOR (47). It would be interesting to elucidate whether CPT downregulation of Stat3 phosphorylation is through inhibiting mTOR signaling.

We found CPT inhibited proliferation of Rh30 and DU145 by arresting cells in G_1/G_0 phase of the cell cycle. This is an interesting finding because both Rh30 and DU145 cells express mutant *p53* alleles, losing the function of p53 (38,48). Therefore, it appears that CPT is able to arrest cells in the G_1/G_0 phase in a *p53*-independent manner. Mutations of *p53* have been documented in over 50% human tumors (49). Our findings suggest that CPT may have potential applications as a chemotherapeutic agent against those *p53* mutant tumor cells, which are resistant to irradiation therapy or other chemotherapies. However, we also noticed that CPT inhibits tumor cell proliferation at rather high concentrations, with IC_{50} values (3–5 μM) for Rh30 and DU145 cells. Animal studies have revealed that achievable maximal plasma concentrations of CPT were only 14.7–55.8 ng/ml (i.e. 0.05–0.18 μM) in rats and 3.1–227.4 ng/ml (i.e. 0.01–0.77 μM) in dogs, respectively, after oral administration of a single dose (30–180 mg/kg for rats; 17.8–1080 mg/kg for dogs) of CPT (50). Therefore, it is necessary to develop new formula (such as nanoparticles) of CPT to increase its bioavailability or more potent CPT analogs for cancer prevention and treatment.

Eukaryotic cell-cycle progression is balanced by cyclins/CDKs and CDK inhibitors (1). Early G_1 transition is mainly regulated by cyclin D complexed with CDK4 and/or CDK6, whereas late G_1-S and early S-phase transitions are regulated by cyclin E coupled with CDK2 (1,4,5).

To investigate how CPT arrests cells in G_1/G_0 phase, we examined the effects of CPT on the expression of cell-cycle regulatory proteins. Our Western blot analysis consistently revealed that CPT downregulated protein expression of cyclin D1, but failed to alter expression of cyclin A, cyclin B1, cyclin E, and CDK2 in all cell lines tested, including Rh30 (Fig.3), DU145, and MCF-7 (data not shown). Our results further suggest that CPT downregulation of cyclin D1 expression is due to inhibition of mTOR signaling. This is supported by the findings that overexpression of constitutively active mTOR in Rh30 cells conferred high resistance to CPT inhibition of cyclin D1 expression (Fig.5). Our data are in agreement with previous findings that mTOR controls synthesis of cyclin D1 (43). Taken together, the results suggest that CPT inhibition of mTOR-mediated expression of cyclin D1 may be primarily responsible for G_1/G_0 cell cycle arrest.

In the studies, we found that CPT inhibited mTORC1-mediated phosphorylation of S6K1 and 4E-BP1, but increased mTORC2-mediated phosphorylation of Akt. It has been described that S6K1 phosphorylates insulin receptor substrate 1 (IRS-1), promoting its degradation (51). Inhibition of S6K1 activity prevents phosphorylation of IRS-1 (S636/639), resulting in accumulation of IRS-1 and activation of its downstream kinases, such as PI3K and Akt, by a feedback regulating mechanism (51–54). Our preliminary data indicate that CPT did not alter either protein expression of PI3K (p110 and p85) or phosphorylation of p85 (data not shown**)**. Whether CPT activates Akt through this feedback regulating mechanism remains to be determined. Undoubtedly, it is of greater importance to elucidate how CPT inhibits mTORC1 signaling, as this may provide direct evidence for development of more potent new CPT analogs for cancer prevention and treatment.

The effects of CPT on CDK inhibitors were complex, which appeared to be cell line-dependent. In Rh30, CPT upregulated expression of $p21^{Cip1}$, but downregulated expression of $p27^{Kip1}$; in MCF-7 cells, CPT downregulated expression of $p21^{Cip1}$, but upregulated expression of $p27^{Kip1}$; in DU145 cells, CPT downregulated expression of both $p21^{Cip1}$ and $p27^{Kip1}$ (data not shown). Both Rh30 and DU145 cells express mutant *p53* alleles, and MCF-7 cells express wild type *p53* (38,49), suggesting that CPT upregulation or downregulation of $p21^{Cip1}$ was independent of *p53*. It has been described that inhibition of mTOR results in accumulation of $p27^{Kip1}$ (55) and reduction of $p21^{Cip1}$ expression (56). Further studies may help unveil whether upregulation of $p27^{Kip1}$ and downregulation of $p21^{Cip1}$ expression in MCF-7 or DU145 cells is a consequence of mTOR inhibition.

The Rb tumor-suppressor protein, a major target of CDKs, plays a pivotal role in the regulation of cell cycle progression from G_1 to S phase (2). The activity of Rb is controlled by its phosphorylation status (2). Hypophosphorylated Rb is the active growth-inhibitory form, which binds E2F and prevents G_1/S transition; in contrast, hyperphosphorylated Rb is released from E2F and is the inactive form (2). The D cyclins and their counterparts CDKs have been suggested to be the most important regulators of Rb phosphorylation (2,3). Here we observed a profound loss of Rb phosphorylation after 24 h exposure to CPT in Rh30 cells. Overexpression of constitutively active mTOR rendered high resistance to CPT inhibition of cyclin D1 expression and Rb phosphorylation, further supporting the notion that CPT-induced G_1/G_0 cell cycle arrest is a consequence of suppression of mTOR-mediated cyclin D1 expression and Rb phosphorylation.

In summary, we have shown that CPT inhibits proliferation of tumor cells by arresying cells in G_1/G_0 cell cycle, which is related to downregulation of cyclin D1 expression, resulting in hypophosphorylation of Rb. The anti-proliferative effect of CPT is probably linked to inhibition of mTOR signaling pathway.

Supplementary Material

Refer to Web version on PubMed Central for supplementary material.

Acknowledgments

This work was supported in part by NIH (CA115414; S. Huang), American Cancer Society (RSG-08-135-01-CNE; S. Huang), and National Natural Science Foundation of China (30371727 and 30772766, Y. Lu). We thank Drs. Christopher J. Rhodes and Peter J. Houghton for providing Ad-mTOR-RD and Rh30 cells, respectively.

Grant support: This work was supported in part by NIH (CA115414; S. Huang), American Cancer Society (RSG-08-135-01-CNE; S. Huang), and National Natural Science Foundation of China (30371727 and 30772766, Y. Lu).

References

1. Malumbres M, Barbacid M. Cell cycle, CDKs and cancer: a changing paradigm. Nat Rev Cancer 2009;9:153–166. [PubMed: 19238148]
2. Burkhart DL, Sage J. Cellular mechanisms of tumour suppression by the retinoblastoma gene. Nat Rev Cancer 2008;8:671–682. [PubMed: 18650841]
3. Polager S, Ginsberg D. E2F - at the crossroads of life and death. Trends Cell Biol 2008;18:528–535. [PubMed: 18805009]
4. Santamaria D, Ortega S. Cyclins and CDKS in development and cancer: lessons from genetically modified mice. Front Biosci 2006;11:1164–1188. [PubMed: 16146805]
5. Lindqvist A, Rodríguez-Bravo V, Medema RH. The decision to enter mitosis: feedback and redundancy in the mitotic entry network. J Cell Biol 2009;185:193–202. [PubMed: 19364923]
6. Guertin DA, Sabatini DM. Defining the role of mTOR in cancer. Cancer Cell 2007;12:9–22. [PubMed: 17613433]
7. Fonseca BD, Smith EM, Lee VH, Mackintosh C, Proud CG. PRAS40 is a target for mammalian target of rapamycin complex 1 and is required for signaling downstream of this complex. J Biol Chem 2007;282:24514–24524. [PubMed: 17604271]
8. Hara K, Maruki Y, Long X, et al. Raptor, a binding partner of target of rapamycin (TOR), mediates TOR action. Cell 2002;110:177–189. [PubMed: 12150926]
9. Kim DH, Sarbassov DD, Ali SM, et al. mTOR interacts with raptor to form a nutrient-sensitive complex that signals to the cell growth machinery. Cell 2002;110:163–175. [PubMed: 12150925]
10. Kim DH, Sarbassov DD, Ali SM, et al. GbetaL, a positive regulator of the rapamycin-sensitive pathway required for the nutrient-sensitive interaction between raptor and mTOR. Mol Cell 2003;11:895–904. [PubMed: 12718876]
11. Loewith R, Jacinto E, Wullschleger S, et al. Two TOR complexes, only one of which is rapamycin sensitive, have distinct roles in cell growth control. Mol Cell 2002;10:457–468. [PubMed: 12408816]
12. Sancak Y, Thoreen CC, Peterson TR, et al. PRAS40 is an insulin-regulated inhibitor of the mTORC1 protein kinase. Mol Cell 2007;25:903–915. [PubMed: 17386266]
13. Vander Haar E, Lee SI, Bandhakavi S, Griffin TJ, Kim DH. Insulin signalling to mTOR mediated by the Akt/PKB substrate PRAS40. Nat Cell Biol 2007;9:316–323. [PubMed: 17277771]
14. Fasolo A, Sessa C. mTOR inhibitors in the treatment of cancer. Expert Opin Investig Drugs 2008;17:1717–1734.
15. Frias MA, Thoreen CC, Jaffe JD, et al. mSin1 is necessary for Akt/PKB phosphorylation, and its isoforms define three distinct mTORC2s. Curr Biol 2006;16:1865–1870. [PubMed: 16919458]
16. Jacinto E, Loewith R, Schmidt A, et al. Mammalian TOR complex 2 controls the actin cytoskeleton and is rapamycin insensitive. Nat Cell Biol 2004;6:1122–1128. [PubMed: 15467718]
17. Sarbassov DD, Ali SM, Kim DH, et al. Rictor, a novel binding partner of mTOR, defines a rapamycin-insensitive and raptor-independent pathway that regulates the cytoskeleton. Curr Biol 2004;14:1296–1302. [PubMed: 15268862]

18. Jacinto E, Facchinetti V, Liu D, et al. SIN1/MIP1 maintains rictor-mTOR complex integrity and regulates Akt phosphorylation and substrate specificity. Cell 2006;127:125–137. [PubMed: 16962653]
19. Pearce LR, Huang X, Boudeau J, et al. Identification of Protor as a novel Rictor-binding component of mTOR complex-2. Biochem J 2007;405:513–522. [PubMed: 17461779]
20. Yang Q, Inoki K, Ikenoue T, Guan KL. Identification of Sin1 as an essential TORC2 component required for complex formation and kinase activity. Genes Dev 2006;20:2820–2832. [PubMed: 17043309]
21. Woo SY, Kim DH, Jun CB, et al. PRR5, a novel component of mTOR complex 2, regulates platelet-derived growth factor receptor beta expression and signaling. J Biol Chem 2007;282:25604–25612. [PubMed: 17599906]
22. Sarbassov DD, Guertin DA, Ali SM, Sabatini DM. Phosphorylation and regulation of Akt/PKB by the rictor-mTOR complex. Science 2005;307:1098–1101. [PubMed: 15718470]
23. Dada S, Demartines N, Dormond O. mTORC2 regulates PGE2-mediated endothelial cell survival and migration. Biochem Biophys Res Commun 2008;372:875–879. [PubMed: 18539142]
24. Facchinetti V, Ouyang W, Wei H, et al. The mammalian target of rapamycin complex 2 controls folding and stability of Akt and protein kinase C. EMBO J 2008;27:1932–1943. [PubMed: 18566586]
25. Ikenoue T, Inoki K, Yang Q, Zhou X, Guan KL. Essential function of TORC2 in PKC and Akt turn motif phosphorylation, maturation and signalling. EMBO J 2008;27:1919–1931. [PubMed: 18566587]
26. Cheng TO. Cardiovascular effects of Danshen. Int J Cardiol 2007;121:9–22. [PubMed: 17363091]
27. Zhou L, Zuo Z, Chow MS. Danshen: an overview of its chemistry, pharmacology, pharmacokinetics, and clinical use. J Clin Pharmacol 2005;45:1345–1359. [PubMed: 16291709]
28. Wojcikowski K, Johnson DW, Gobe G. Herbs or natural substances as complementary therapies for chronic kidney disease: ideas for future studies. J Lab Clin Med 2006;147:160–166. [PubMed: 16581343]
29. Wang BE. Treatment of chronic liver diseases with traditional Chinese medicine. J Gastroenterol Hepatol 2000;15 Suppl:E67–E70. [PubMed: 10921385]
30. Yu XY, Lin SG, Chen X, et al. Transport of cryptotanshinone, a major active triterpenoid in Salvia miltiorrhiza Bunge widely used in the treatment of stroke and Alzheimer's disease, across the blood-brain barrier. Curr Drug Metab 2007;8:365–378. [PubMed: 17504224]
31. Jin DZ, Yin LL, Ji XQ, Zhu XZ. Cryptotanshinone inhibits cyclooxygenase-2 enzyme activity but not its expression. Eur J Pharmacol 2006;549:166–172. [PubMed: 16989810]
32. Suh SJ, Jin UH, Choi HJ, et al. Cryptotanshinone from Salvia miltiorrhiza BUNGE has an inhibitory effect on TNF-alpha-induced matrix metalloproteinase-9 production and HASMC migration via down-regulated NF-kappaB and AP-1. Biochem Pharmacol 2006;72:1680–1689. [PubMed: 16999937]
33. Kim EJ, Jung SN, Son KH, et al. Antidiabetes and antiobesity effect of cryptotanshinone via activation of AMP-activated protein kinase. Mol Pharmacol 2007;72:62–72. [PubMed: 17429005]
34. Don MJ, Liao JF, Lin LY, Chiou WF. Cryptotanshinone inhibits chemotactic migration in macrophages through negative regulation of the PI3K signaling pathway. Br J Pharmacol 2007;151:638–646. [PubMed: 17471173]
35. Zhang F, Zheng W, Pi R, et al. Cryptotanshinone protects primary rat cortical neurons from glutamate-induced neurotoxicity via the activation of the phosphatidylinositol 3-kinase/Akt signaling pathway. Exp Brain Res 2008;193:109–118. [PubMed: 18936923]
36. Nizamutdinova IT, Lee GW, Son KH, et al. Tanshinone I effectively induces apoptosis in estrogen receptor-positive (MCF-7) and estrogen receptor-negative (MDA-MB-231) breast cancer cells. Int J Oncol 2008;33:485–491. [PubMed: 18695877]
37. Shin DS, Kim HN, Shin KD, et al. Cryptotanshinone inhibits constitutive signal transducer and activator of transcription 3 function through blocking the dimerization in DU145 prostate cancer cells. Cancer Res 2009;69:193–202. [PubMed: 19118003]
38. Beevers CS, Li F, Liu L, Huang S. Curcumin inhibits the mammalian target of rapamycin-mediated signaling pathways in cancer cells. Int J Cancer 2006;119:757–764. [PubMed: 16550606]

39. Coward P, Wada HG, Falk MS, et al. Controlling signaling with a specifically designed Gi-coupled receptor. Proc Natl Acad Sci USA 1998;95:352–357. [PubMed: 9419379]
40. Briaud I, Dickson LM, Lingohr MK, McCuaig JF, Lawrence JC, Rhodes CJ. Insulin receptor substrate-2 proteasomal degradation mediated by a mammalian target of rapamycin (mTOR)-induced negative feedback down-regulates protein kinase B-mediated signaling pathway in beta-cells. J Biol Chem 2005;280:2282–2293. [PubMed: 15537654]
41. Liu L, Chen L, Chung J, Huang S. Rapamycin inhibits F-actin reorganization and phosphorylation of focal adhesion proteins. Oncogene 2008;27:4998–5010. [PubMed: 18504440]
42. Liu L, Li F, Cardelli JA, Martin KA, Blenis J, Huang S. Rapamycin inhibits cell motility by suppression of mTOR-mediated S6K1 and 4E-BP1 pathways. Oncogene 2006;25:7029–7040. [PubMed: 16715128]
43. Hashemolhosseini S, Nagamine Y, Morley SJ, Desrivieres S, Mercep L, Ferrari S. Rapamycin inhibition of the G1 to S transition is mediated by effects on cyclin D1 mRNA and protein stability. J Biol Chem 1998;273:14424–14429. [PubMed: 9603954]
44. Chen Y, Knudsen ES, Wang JY. The RB/p107/p130 phosphorylation pathway is not inhibited in rapamycin-induced G1-prolongation of NIH3T3 cells. Oncogene 1996;13:1765–1771. [PubMed: 8895523]
45. Brunn GJ, Hudson CC, Sekulić A, et al. Phosphorylation of the translational repressor PHAS-I by the mammalian target of rapamycin. Science 1997;277:99–101. [PubMed: 9204908]
46. Holz MK, Blenis J. Identification of S6 kinase 1 as a novel mammalian target of rapamycin (mTOR)-phosphorylating kinase. J Biol Chem 2005;280:26089–26093. [PubMed: 15905173]
47. Zhou J, Wulfkuhle J, Zhang H, et al. Activation of the PTEN/mTOR/STAT3 pathway in breast cancer stem-like cells is required for viability and maintenance. Proc Natl Acad Sci USA 2007;104:16158–16163. [PubMed: 17911267]
48. Isaacs WB, Carter BS, Ewing CM. Wild-type p53 suppresses growth of human prostate cancer cells containing mutant p53 alleles. Cancer Res 1991;51:4716–4720. [PubMed: 1873816]
49. Levine AJ. p53, the cellular gatekeeper for growth and division. Cell 1997;88:323–331. [PubMed: 9039259]
50. Pan Y, Bi HC, Zhong GP, et al. Pharmacokinetic characterization of hydroxylpropyl-beta-cyclodextrin-included complex of cryptotanshinone, an investigational cardiovascular drug purified from Danshen (Salvia miltiorrhiza). Xenobiotica 2008;38:382–398. [PubMed: 18340563]
51. Tremblay F, Marette A. Amino acid and insulin signaling via the mTOR/p70 S6 kinase pathway. A negative feedback mechanism leading to insulin resistance in skeletal muscle cells. J Biol Chem 2001;276:38052–38060. [PubMed: 11498541]
52. Tzatsos A, Kandror KV. Nutrients suppress phosphatidylinositol 3-kinase/Akt signaling via raptor-dependent mTOR-mediated insulin receptor substrate 1 phosphorylation. Mol Cell Biol 2006;26:63–76. [PubMed: 16354680]
53. O'Reilly KE, Rojo F, She QB, et al. mTOR inhibition induces upstream receptor tyrosine kinase signaling and activates Akt. Cancer Res 2006;66:1500–1508. [PubMed: 16452206]
54. Wan X, Harkavy B, Shen N, Grohar P, Helman LJ. Rapamycin induces feedback activation of Akt signaling through an IGF-1R-dependent mechanism. Oncogene 2007;26:1932–1940. [PubMed: 17001314]
55. Nourse J, Firpo E, Flanagan WM, et al. Interleukin-2-mediated elimination of the $p27^{Kip1}$ cyclin-dependent kinase inhibitor prevented by rapamycin. Nature 1994;372:570–573. [PubMed: 7990932]
56. Beuvink I, Boulay A, Fumagalli S, et al. The mTOR inhibitor RAD001 sensitizes tumor cells to DNA-damaged induced apoptosis through inhibition of p21 translation. Cell 2005;120:747–759. [PubMed: 15797377]

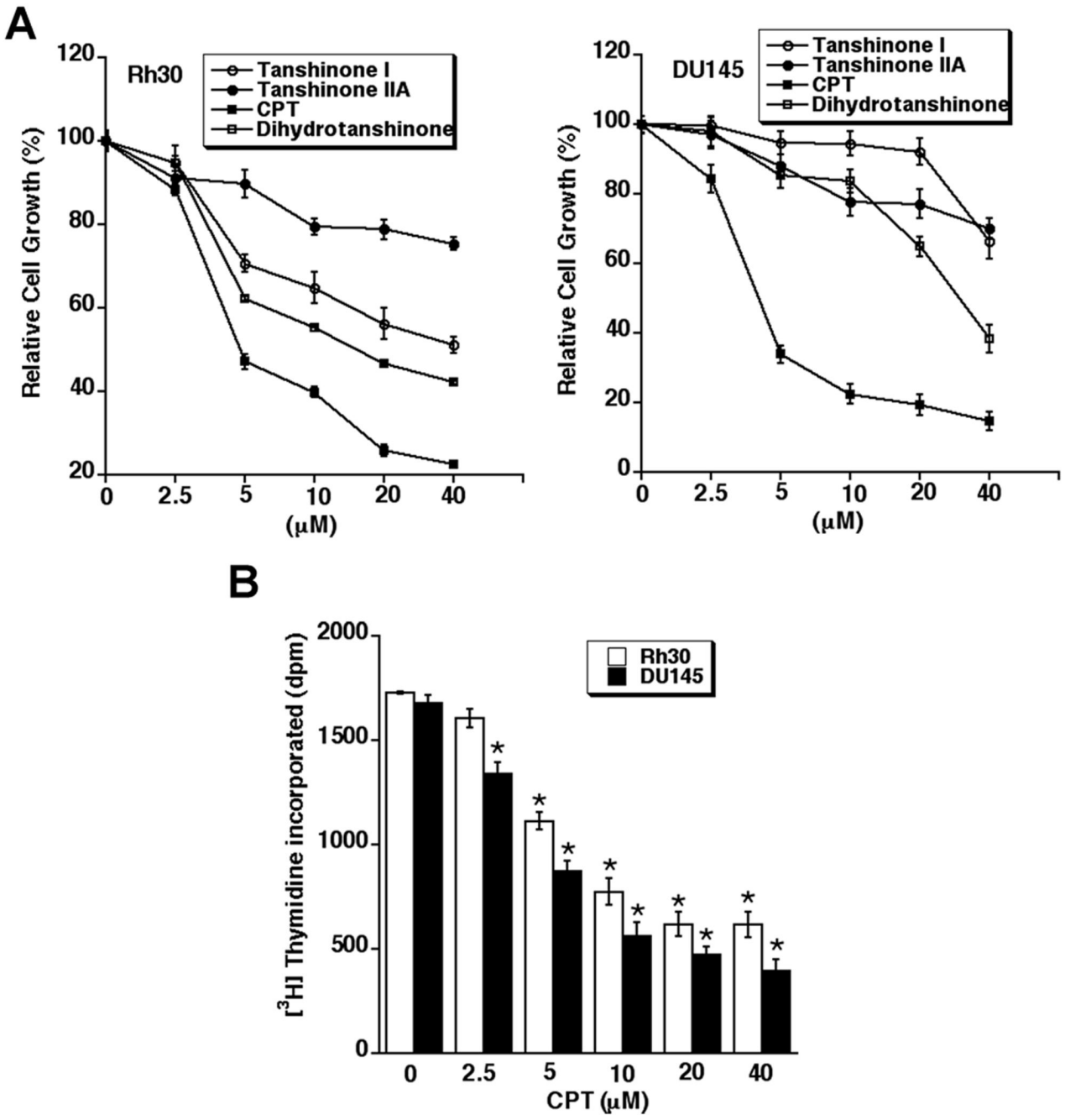

Fig. 1. CPT inhibits proliferation of cancer cells in a concentration-dependent manner

Rh30 and DU145, grown in 96-well plates with RPMI 1640 medium supplemented with 10% FBS, were exposed to indicated compounds (0–40 μM) for 48 h. Cell proliferation was evaluated using One solution cell proliferation assay (A) or [^{3}H]Thymidine incorporation assay (B), as described in *Materials and Methods*. Results in (A) and (B) are presented as mean ± SE (n = 3). **P* < 0.05, difference vs. control.

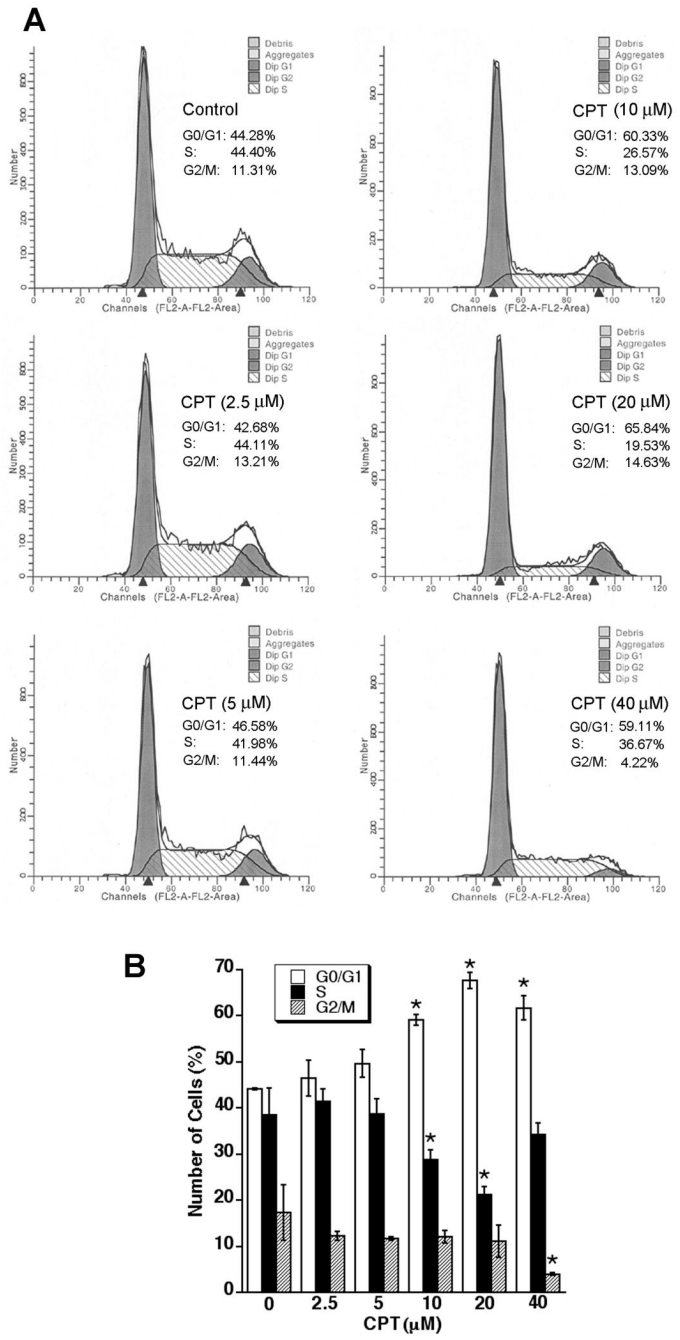

Fig. 2. CPT arrests cell cycle in G_1/G_0 phase in cancer cells

(A, B) Rh30 cells, grown in 6-well plates (1×10^5 cells/well) with RPMI 1640 medium supplemented with 10% FBS, were treated with CPT (0–40 μM) for 24 h, followed by cell cycle analysis using Cellular DNA Flow Cytometric Analysis Kit. (A) A representative cell cycle analysis result for Rh30 cells is shown. (B) Results are presented as mean ± SE (n = 3). **P* < 0.05, difference *vs.* control.

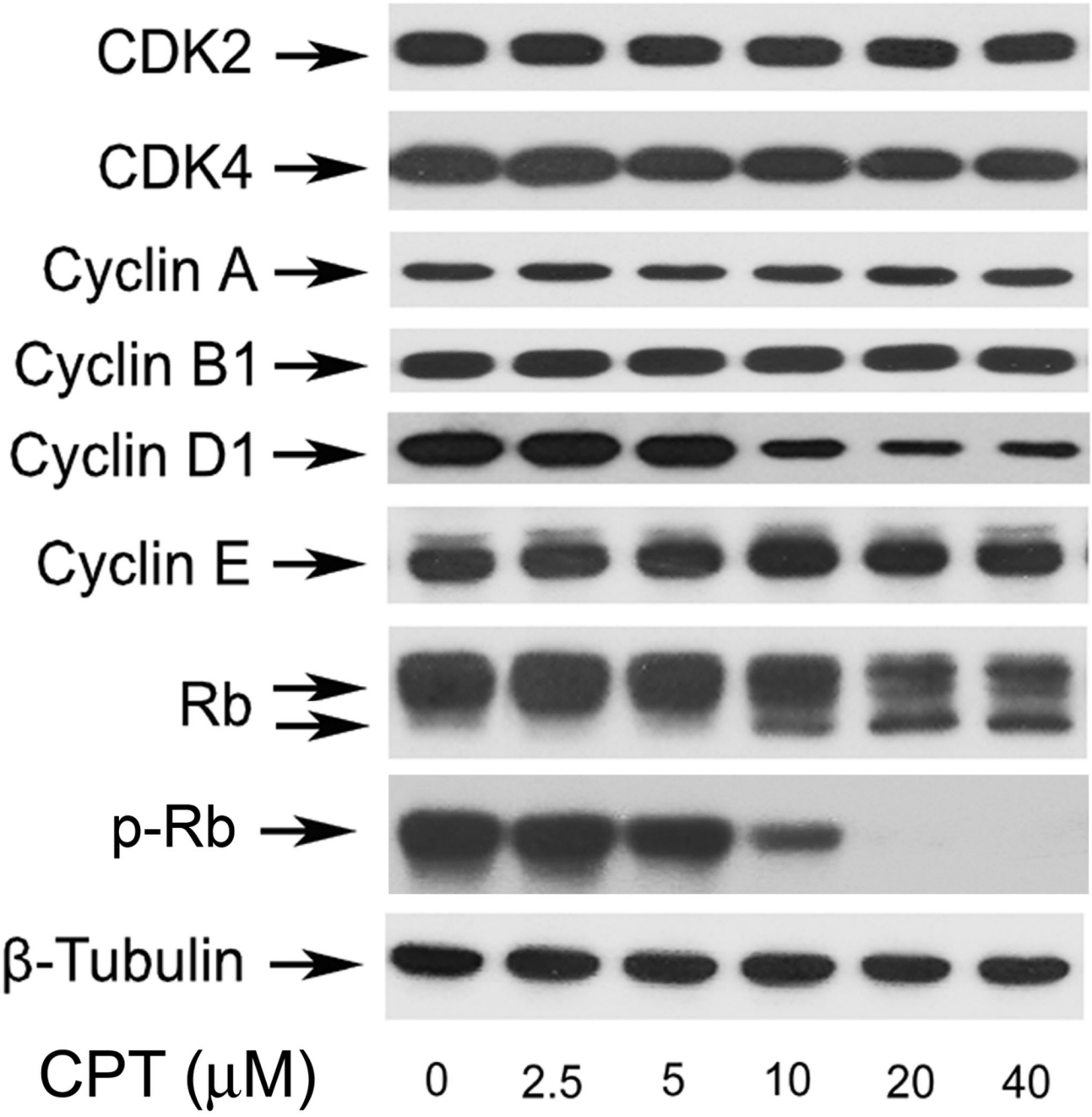

Fig. 3. CPT inhibits cyclin D1 expression and Rb phosphorylation in cancer cells

Rh30 cells were treated with CPT (0–40 μM) for 24 h, followed by Western blotting with indicated antibodies. β-Tubulin was used for loading control.

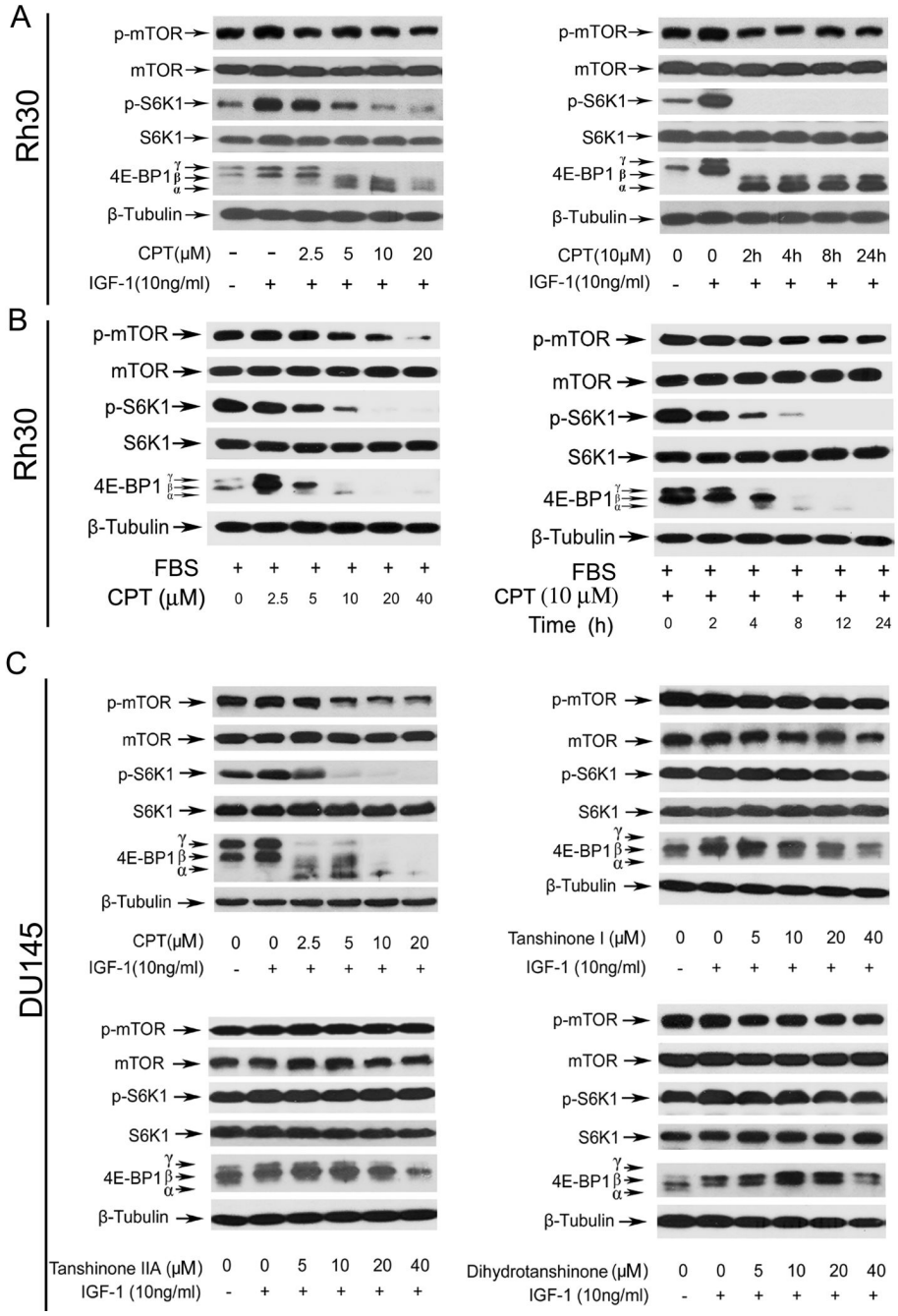

Fig. 4. CPT inhibits mTOR pathway in cancer cells

Western blot analysis was performed for (A–D). β-Tubulin was used for loading control. Serum-starved (A) or non-starved Rh30 cells (B) were pre-treated with CPT (0–40 μM) for 2 h, and then stimulated with IGF-1 (10 ng/ml) for 1 h (Left Panel), or with CPT (10 μM) for the indicated time and stimulated with IGF-1 (10 ng/ml) for 1 h (Right Panel). (C) Serum-starved DU145 cells were treated with CPT, tanshinone I, tanshinone IIA or dihydrotanshinone (0–40 μM), respectively, for 2 h, and then stimulated with IGF-1 (10 ng/ml) for 1 h.

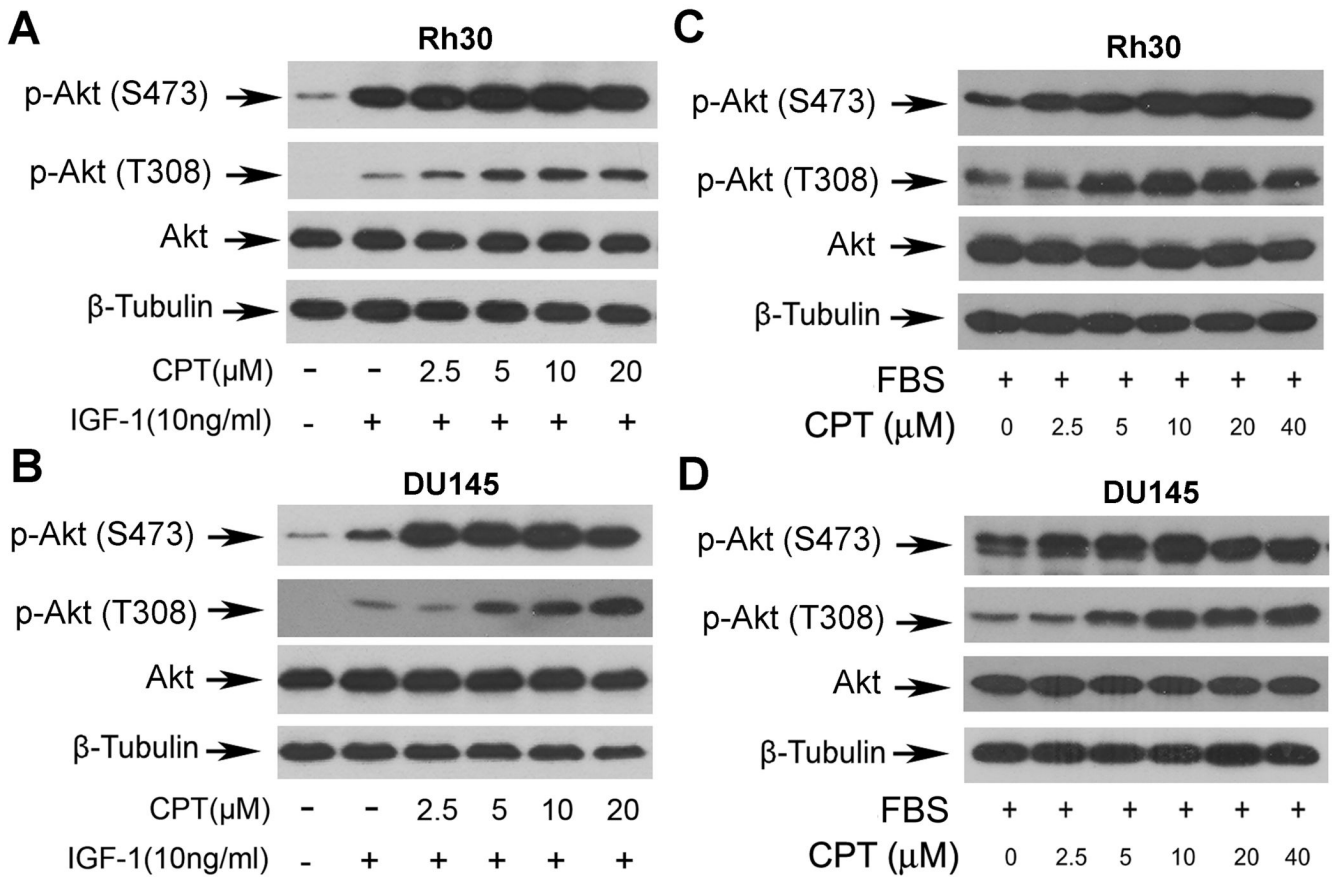

Fig. 5. CPT activates Akt in a concentration-dependent manner

Serum-starved (A,B) or non-starved (C,D) Rh30 and DU145 cells were pre-treated with CPT (0–40 μM) for 2 h, and then stimulated with (A,B) or without (C,D) IGF-1 (10 ng/ml) for 1 h. The cell lysates were subjected to Western blot analysis with indicated antibodies. β-Tubulin was used for loading control.

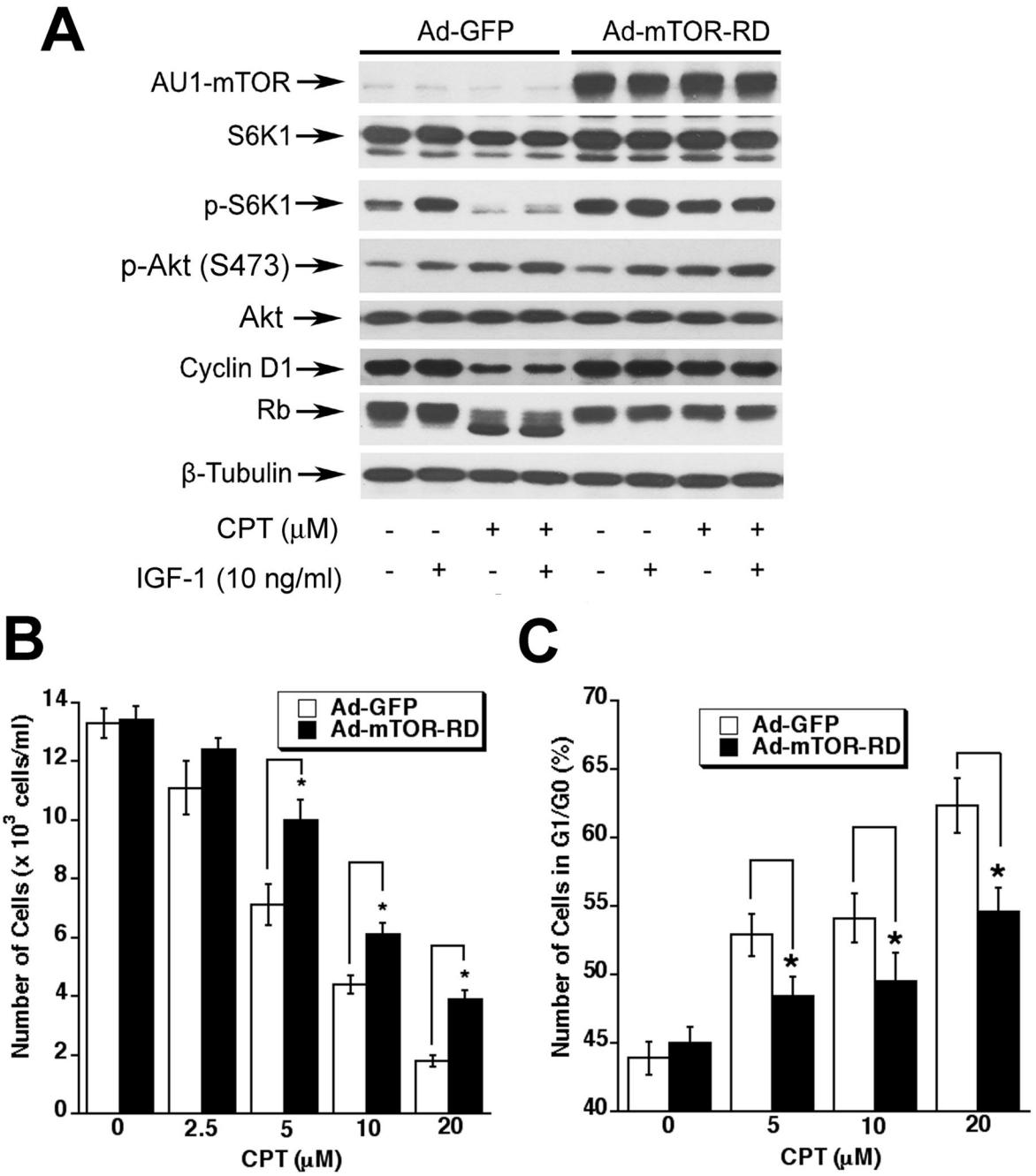

Fig. 6. Expression of constitutively active mTOR confers high resistance to CPT inhibition of mTOR signaling, cyclin D1 expression and Rb phosphoryaltion, and partially prevents CPT inhibition of cell proliferation in cancer cells

(A) Rh30 cells, grown in 6-well plates and infected with Ad-GFP or Ad-mTOR-RD for 24 h, and treated with or without CPT (10 μM) for 2 h, followed by stimulation with or without IGF-1 (10 ng/ml) for 1 h. The cell lysates were subjected to Western blot analysis with indicated antibodies. β-Tubulin was used for loading control. (B,C) Rh30 cells, grown in 6-well plates and infected with Ad-GFP or Ad-mTOR-RD for 24 h, were treated with CPT (0–20 μM) respectively for 24 h, followed by cell counting using a Beckman Coulter Counter (B), or cell cycle analysis (C). Results are presented as mean ± SE (n = 3). **P* < 0.05, difference *vs.* control.